

AD-A098 425

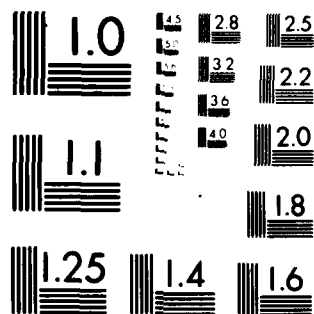
ROCKWELL INTERNATIONAL THOUSAND OAKS CA SCIENCE CENTER F/8 11/2  
RESEARCH OF MICROSTRUCTURALLY DEVELOPED TOUGHENING MECHANISMS I--ETC(U)  
MAR 81 F F LANGE N00014-77-C-0841

UNCLASSIFIED

SC5117.12TR

NL

END  
DATE  
FILMED  
5 81  
DTIC



MICROCOPY RESOLUTION TEST CHART  
NATIONAL BUREAU OF STANDARDS-1963-A

LEVEL III

(2)



Rockwell International  
Science Center  
SC5117.12TR

*Cal 1980*

TRANSFORMATION TOUGHENING

PART 5: EFFECT OF TEMPERATURE AND ALLOY ON FRACTURE TOUGHNESS

*MAT-81*

F.F. Lange

Structural Ceramics Group  
Rockwell International Science Center  
Thousand Oaks, California 91360

ABSTRACT

*NOO 14-77-C-0441*

AD A098425

The critical stress intensity factor ( $K_{IC}$ ) of materials containing tetragonal  $ZrO_2$  was found to decrease with increasing temperature and  $CeO_2$  alloying additions, as predicted by theory. The temperature dependence of  $K_{IC}$  was related to the temperature dependence of the chemical free energy change associated with the tetragonal + monoclinic transformation. Good agreement with thermodynamic data available for pure  $ZrO_2$  was obtained when the size of the transformation zone associated with the crack was equated to the size of the  $ZrO_2$  grains. The  $K_{IC}$  vs  $CeO_2$  addition data was used to estimate the tetragonal, monoclinic, cubic eutectoid temperature of 270°C in the  $ZrO_2$ - $CeO_2$  binary system.

DTIC FILE COPY

Accession For	
NTIS GRA&I	<input checked="" type="checkbox"/>
DTIC TAB	<input type="checkbox"/>
Unannounced	<input type="checkbox"/>
Justifications	
<i>By Order for</i>	
By	
Distribution/	
Availability Codes	
Avail and/or	Special
<i>A</i>	

DTIC  
ELECTE

MAY 4 1981

A

This document has been approved  
for public release and sale; its  
distribution is unlimited.

1  
C2707A/jbs

81 5 04 116

UNCLASSIFIED

SECURITY CLASSIFICATION OF THIS PAGE (When Data Entered)

(12) 21

REPORT DOCUMENTATION PAGE		READ INSTRUCTIONS BEFORE COMPLETING FORM
1. REPORT NUMBER	2. GOVT ACCESSION NO.	3. RECIPIENT'S CATALOG NUMBER
	AD-A098425	
4. TITLE (and Subtitle)	5. TYPE OF REPORT & PERIOD COVERED	
(6) Research of Microstructurally Developed Toughening Mechanisms in Ceramics, Part 5.	Technical Report No. 12 12/01/80 through 04/01/81	
Effect of Temperature and	6. PERFORMING ORG. REPORT NUMBER	
(10) F.F./Lange Alloy in Fracture Toughness.	(14) SC5117.12TR	
	7. AUTHOR	
	(15) N00014-77-C-0441	
8. PERFORMING ORGANIZATION NAME AND ADDRESS	9. PROGRAM ELEMENT, PROJECT, TASK AREA & WORK UNIT NUMBERS	
Rockwell International Science Center 1049 Camino dos Rios Thousand Oaks, CA 91360	032-574(471)	
11. CONTROLLING OFFICE NAME AND ADDRESS	12. REPORT DATE	
Director, Metallurgy Programs, Material Sciences Office of Naval Research, 800 N. Quincy Street Arlington, VA 22217	(11) March 1981	
13. MONITORING AGENCY NAME & ADDRESS (if different from Controlling Office)	14. NUMBER OF PAGES	
(9) Technical rept no. 12 1 Dec 80-1 Apr 81	21	
15. DISTRIBUTION STATEMENT (of this Report)	16. SECURITY CLASS. (of this report)	
Approved for public release; distribution unlimited	Unclassified	
17. DISTRIBUTION STATEMENT (of the abstract entered in Block 20, if different from Report)	18a. DECLASSIFICATION/DOWNGRADING SCHEDULE	
19. SUPPLEMENTARY NOTES		
20. KEY WORDS (Continue on reverse side if necessary and identify by block number)		
Fracture toughness, martensitic transformations, ZrO <sub>2</sub> , Al <sub>2</sub> O <sub>3</sub> , phase transformation, strength		
21. ABSTRACT (Continue on reverse side if necessary and identify by block number)		
The critical stress intensity factor ( $K_{IC}$ ) of materials containing tetragonal ZrO <sub>2</sub> was found to decrease with increasing temperature and CeO <sub>2</sub> alloying additions, as predicted by theory. The temperature dependence of $K_{IC}$ was related to the temperature dependence of the chemical free energy change associated with the tetragonal to monoclinic transformation. Good agreement with thermodynamic data available for pure ZrO <sub>2</sub> was obtained when the size of the transformation zone associated with the crack was equated to the size		

DD FORM 1473

EDITION OF 1 NOV 65 IS OBSOLETE

UNCLASSIFIED

SECURITY CLASSIFICATION OF THIS PAGE (When Data Entered)

yields

389949

UNCLASSIFIED

SECURITY CLASSIFICATION OF THIS PAGE(When Data Entered)

of the  $ZrO_2$  grains. The  $K_C$  vs  $CeO_2$  addition data was used to estimate the tetragonal, monoclinic, cubic eutectoid temperature of  $270^\circ C$  in the  $ZrO_2$ - $CeO_2$  binary system.

7

UNCLASSIFIED

SECURITY CLASSIFICATION OF THIS PAGE(When Data Entered)



## 1.0 INTRODUCTION

In Part 2,<sup>(1)</sup> theory was presented showing that the contribution to fracture toughness ( $K_C$ ) by a stress-induced transformation is proportional to the chemical free energy change ( $|\Delta G^C|$ ) associated with the transformation. For the  $ZrO_2$  (tetragonal)  $\rightarrow$   $ZrO_2$  (monoclinic) transformation,  $|\Delta G^C|$  is known to decrease with increasing temperature and with alloying  $ZrO_2$  with  $Y_2O_3$ ,  $CeO_2$  etc. In this part of the series, experiments were designed to measure  $K_C$  as a function of temperature and alloy content. The temperature dependence of  $K_C$  was measured on polycrystalline  $ZrO_2$  and two-phase  $Al_2O_3/ZrO_2$  materials in which 2 m/o  $Y_2O_3$  was alloyed with the  $ZrO_2$ . The fabrication conditions and general properties of these materials have been reported in Part 4.<sup>2</sup>

A series of  $Al_2O_3/ZrO_2$  materials in which  $CeO_2$  was alloyed with the  $ZrO_2$  phase was used to determine the effect of alloy content on  $K_C$ . As shown in Fig. 1,  $CeO_2$  was a good candidate for this study since it forms an extensive solid-solution, tetragonal  $ZrO_2$  phase field and lowers the tetragonal  $\rightarrow$  monoclinic transformation temperature to  $< 25^\circ C$  at  $\sim 20$  m/o  $CeO_2$ .<sup>\*</sup> Initial  $ZrO_2$ - $CeO_2$  sintering studies were not successful, i.e., higher  $CeO_2$  contents (added to  $ZrO_2$  powder as a soluble nitrate) resulted in a low density material. Hot-pressing was avoided, since  $CeO_2$  reduces to  $Ce_2O_3$  in environments produced by graphite dies. Attempts to sinter  $Al_2O_3/30$  v/o  $ZrO_2$  composite powders containing  $CeO_2$  were successful in terms of density and phase content. Thus, these

<sup>\*</sup>In contrast, the working tetragonal phase field with  $Y_2O_3$  additions is limited to compositions between 2 and 3 m/o  $Y_2O_3$  in both single phase tetragonal  $ZrO_2$  and  $Al_2O_3/ZrO_2$  compositions.<sup>2</sup>



SC81-11656

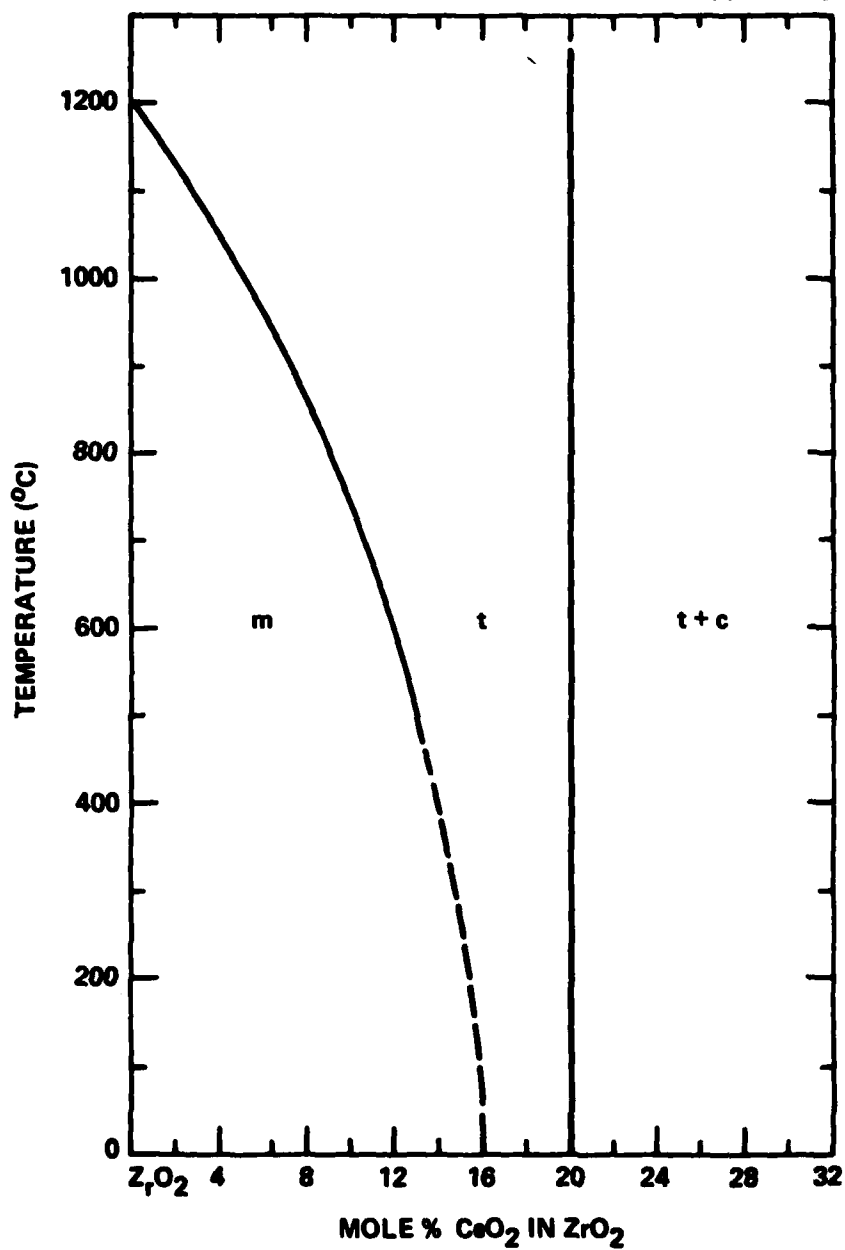


Fig. 1 A portion of the ZrO<sub>2</sub>-CeO<sub>2</sub> phase diagram.<sup>5</sup>



composite materials were chosen for the fracture toughness vs alloying content studies.

## 2.0 EXPERIMENTAL

### 2.1 Temperature Dependence

Four materials were chosen for this study. Three of these were hot-pressed as detailed in Part 4:<sup>2</sup>  $\text{Al}_2\text{O}_3/29.5$  v/o  $\text{ZrO}_2$  (+2 m/o  $\text{Y}_2\text{O}_3$ ),  $\text{Al}_2\text{O}_3/45$  v/o  $\text{ZrO}_2$  (+2 m/o  $\text{Y}_2\text{O}_3$ ) and  $\text{ZrO}_2$  (+2 m/o  $\text{Y}_2\text{O}_3$ ). The fourth material was a  $\text{Al}_2\text{O}_3/30$  v/o  $\text{ZrO}_2$  (+2 m/o  $\text{Y}_2\text{O}_3$ ) composite sintered to 97% of theoretical density in air at  $1600^\circ\text{C}/1$  hr in which  $\text{ZrO}_2$  was retained in its tetragonal state. The composite powders were prepared for sintering by mixing the required weight fractions of  $\text{Al}_2\text{O}_3$ ,\*  $\text{ZrO}_2$ \*\* and yttrium nitrate\*\*\* by ball milling in methanol ( $\text{Al}_2\text{O}_3$  balls and plastic bottle), drying, calcining at  $500^\circ\text{C}/4$  hrs, and isostatic pressing at 350 MPa. Small bar specimens cut from each material were polished in preparation for  $K_{\text{IC}}$  measurements.

The indentation technique, developed by Evans and Charles,<sup>4</sup> was used to measure  $K_{\text{IC}}$  over the range of  $-196^\circ\text{C}$  (liquid nitrogen) to  $700^\circ\text{C}$ . A Vickers diamond indenter mounted in tungsten carbide was used with the device which maintained a constant specimen temperature within the range noted. The device consisted of an internally heated copper post, mounted within a metal flask. The flask was attached to an x-y stage used to translate the specimen relative

\*Lindy B, Union Carbide Corp.

\*\*Zircar, Corp.

\*\*\*Research Chemicals Corp.





to the indenter. The stage was mounted on top of a local cell and was insulated from the flask with a machinable ceramic. The specimen was spring-clip loaded in a copper well attached to the post. A chromel-alumel thermocouple, spring-clip loaded to the external face of the specimen, was used to record temperatures. For the  $K_C$  measurements at temperatures  $< 25^\circ\text{C}$ , the flask was externally insulated and filled with liquid nitrogen. The nitrogen was allowed to slowly evaporate to achieve the desired specimen temperature. For measurements at higher temperatures, the flask was filled with insulating ceramic fiber, and the internal heater was controlled to achieve the desired temperature. Argon was forced into the metal flask to protect the copper parts and diamond from oxidation. Between measurements the indenter was held just above the specimen to avoid a large temperature differential when the indenter was again forced into the specimen at 20 Kgms. A single specimen was used for the complete temperature range investigated; two measurements were made at each temperatures.

Flexural strength measurements were made with one of the hot-pressed materials  $[\text{Al}_2\text{O}_3/29.5 \text{ v/o } \text{ZrO}_2 (+2 \text{ m/o } \text{Y}_2\text{O}_3)]$  over the temperature range in which  $K_C$  measurements were made. Bar specimens ( $0.3 \times 0.6 \times > 3.0 \text{ cm}$ ) were diamond cut and ground and then annealed at  $1300^\circ\text{C}$  for 24 hr to eliminate the surface compressive stresses developed due to the transformation of surface material during grinding.<sup>2</sup> Three strength measurements were made in liquid nitrogen, a mixture of dry ice and methanol, room temperature and in air at higher temperatures.



### 2.3 Effect of Alloying

As indicated above, a series of  $\text{Al}_2\text{O}_3/30$  v/o  $\text{ZrO}_2$  composite materials in which  $\text{CeO}_2$  was incorporated were found suitable for fracture toughness vs alloying content studies. Composite powders containing the appropriate weight fractions of  $\text{Al}_2\text{O}_3$ \*,  $\text{ZrO}_2$ \*\* and  $\text{CeO}_2$ \*\*\* were mixed and milled together in plastic bottles containing methanol and  $\text{Al}_2\text{O}_3$  mill balls, dried by flash evaporation, calcined at  $500^\circ\text{C}/16$  hr, isostatically pressed into plates and sintered at  $1600^\circ\text{C}/1$  hr. Sixteen compositions containing a  $\text{CeO}_2$  content between 6 to 22 m/o  $\text{CeO}_2$  were fabricated. Densities of these composites ranged between 94% and 98% of theoretical, based on the density of tetragonal  $\text{ZrO}_2$  calculated using the lattice parameter of  $a = 5.126$  Å and  $c = 5.224$  Å reported by Duwez and Odell.<sup>5</sup> X-ray diffraction analysis of the sintered surfaces showed that 100% of the  $\text{ZrO}_2$  was retained in its tetragonal structure for compositions containing  $> 12$  m/o  $\text{CeO}_2$ . Trace amounts of cubic  $\text{ZrO}_2$  were observed for compositions containing 21 and 22 m/o  $\text{CeO}_2$ , consistent with previous phase equilibria studies.<sup>5</sup> Increasing amounts of monoclinic  $\text{ZrO}_2$  were observed as the  $\text{CeO}_2$  content decreased from 11 m/o to 6 m/o. Based on these observations, composites containing  $> 11$  m/o  $\text{CeO}_2$  were cut and polished for fracture toughness measurements at room temperature as described above.

---

\*Lindy B, Union Carbide Corp.

\*\*Sub-micron  $\text{ZrO}_2$ , Zircar Corp.

\*\*\*Added as Cerrium Nitrate, Research Chemicals Corp.



### 3.0 RESULTS

#### 3.1 Temperature Dependence

Figure 2 illustrates that the fracture toughness decreases with increasing temperature for the four materials investigated. High, low and average values of  $K_C$  are defined by the scatter bar at each temperature. These data were fit to a linear equation:

$$K_C = A - mT \quad , \quad (1)$$

where  $T$  is temperature in degrees centigrade and the constants  $A$  and  $m$  are given in Table 1.

Table 1  
Constants Defining Temperature Dependence of  $K_C$

Material	Fabrication Conditions	A (MPa·m <sup>1/2</sup> )	m (MPa·m <sup>1/2</sup> C <sup>-1</sup> )	Correlation Coefficient
Al <sub>2</sub> O <sub>3</sub> /29.3 v/o ZrO <sub>2</sub> (+2 m/o Y <sub>2</sub> O <sub>3</sub> )	Hot-Pressed 1600°C/1 hr	7.56	0.0044	0.95
Al <sub>2</sub> O <sub>3</sub> /45 v/o ZrO <sub>2</sub> (+2 m/o Y <sub>2</sub> O <sub>3</sub> )	Hot-Pressed 1600°C/1 hr	6.78	0.0029	0.92
ZrO <sub>2</sub> (+2 m/o Y <sub>2</sub> O <sub>3</sub> )	Hot-Pressed 1600°C/1 hr	8.40	0.0041	0.99*
Al <sub>2</sub> O <sub>3</sub> /30 v/o ZrO <sub>2</sub> (+2 m/o Y <sub>2</sub> O <sub>3</sub> )	Sintered 1600°C/1 hr	9.96	0.0054	0.97

\*Data at 100°C excluded.

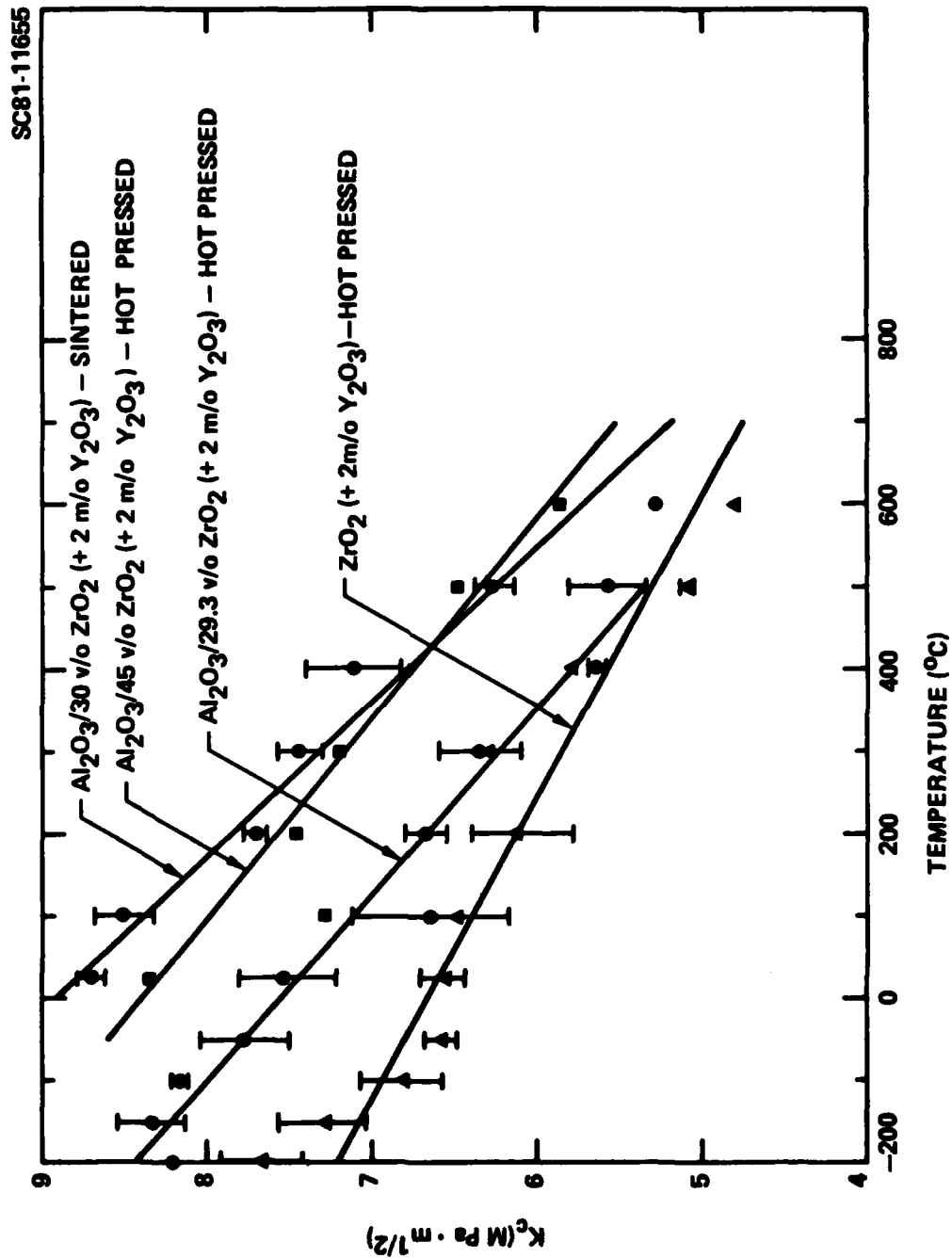


Fig. 2 Critical stress intensity factor vs temperature for the four materials in stigated.



The flexural strength data for the  $\text{Al}_2\text{O}_3/29.3 \text{ v/o ZrO}_2 (+2 \text{ m/o Y}_2\text{O}_3)$  composites are shown in Fig. 3. These data show that strength decreases with increasing temperature. The dashed line illustrates the expected temperature behavior of strength, based on the temperature behavior of  $K_C$  as reported in Table 1 for this composition and normalizing all data to the room temperature value.

### 3.2 Effect of Alloying

Figure 4 reports the  $K_C$  data vs the  $\text{CeO}_2$  addition to the  $\text{ZrO}_2$  in the  $\text{Al}_2\text{O}_3/30 \text{ v/o ZrO}_2$  sintered materials. Data obtained for the composition containing 11 m/o  $\text{CeO}_2$  is low due to its substantial ( $\sim 30 \%$ ) monoclinic  $\text{ZrO}_2$  content. Over the range where only the tetragonal  $\text{ZrO}_2$  phase is observed (12-20 m/o  $\text{CeO}_2$ ),  $K_C$  decreases with increasing  $\text{CeO}_2$  content.  $K_C$  appears to level off to  $\sim 6 \text{ MPa}\cdot\text{m}^{1/2}$  at the reported tetragonal/cubic phase boundary (compositions containing  $> 20 \text{ m/o CeO}_2$ ). A linear relation was assumed over the range of 12-20 m/o  $\text{CeO}_2$ , resulting in the relation:

$$K_C = (10.32 - 0.202 M) \text{ MPa} \cdot \text{m}^{1/2} \quad , \quad (2)$$

where  $M = \text{mole\% CeO}_2$ .

## 4.0 DISCUSSION

In Part 2<sup>1</sup> of this series, it was shown that the fracture toughness of a brittle material containing a phase which would undergo a stress-induced

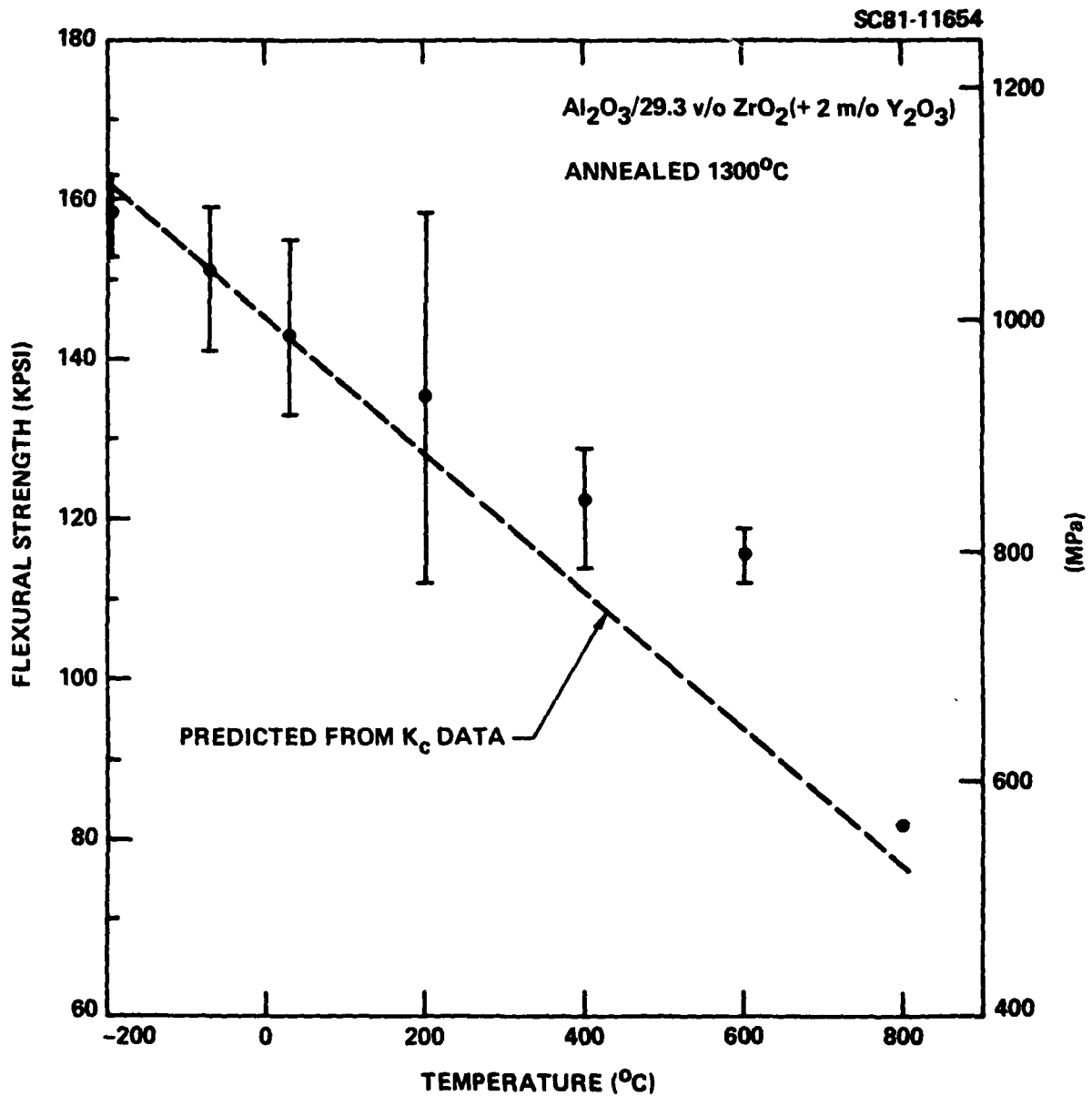


Fig. 3 Flexural strength vs temperature for the  $\text{Al}_2\text{O}_3/29.3 \text{ v/o ZrO}_2(+2 \text{ m/o Y}_2\text{O}_3)$  material. Specimens first annealed at  $1300^\circ\text{C}/24 \text{ hrs.}$

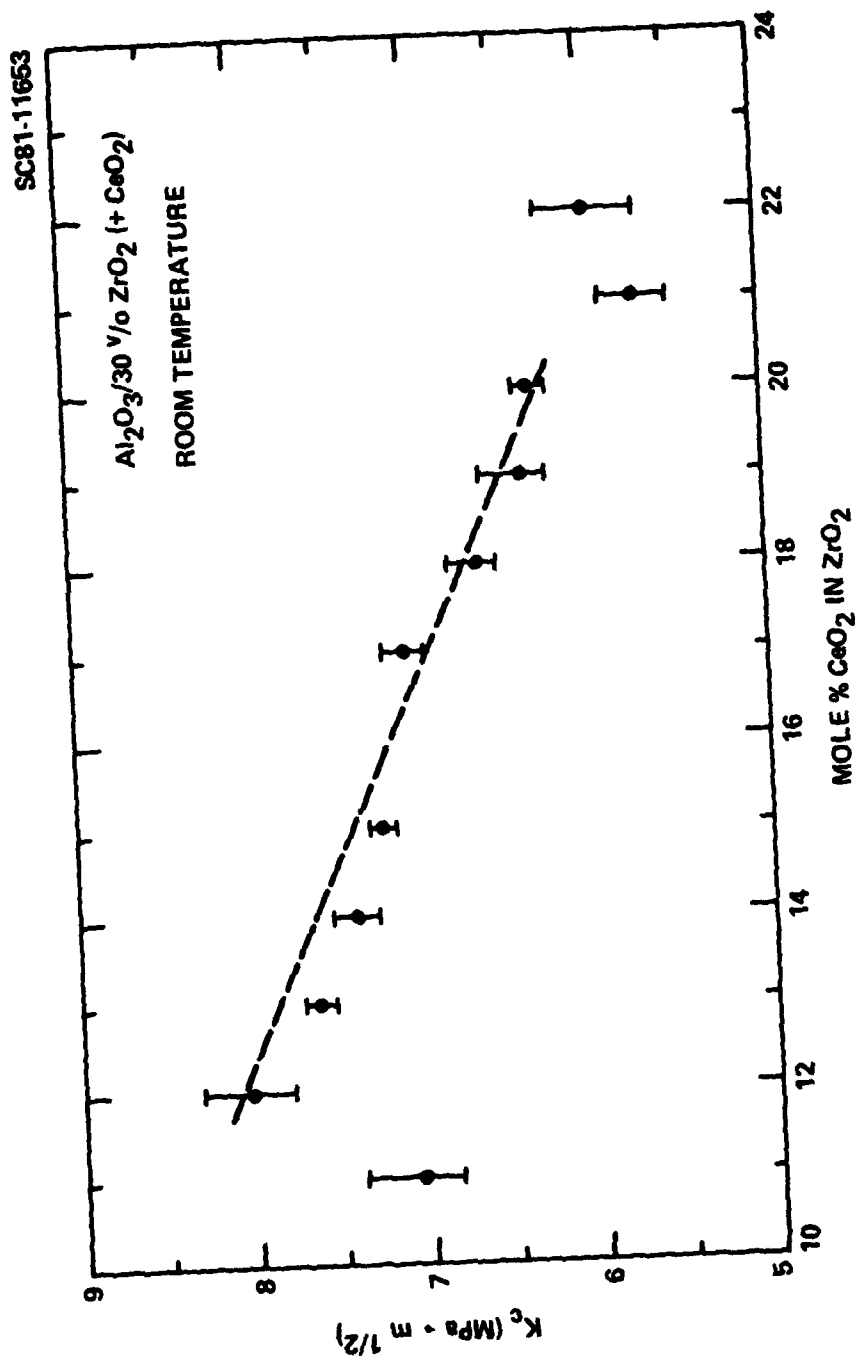


Fig. 4 Critical stress intensity factor vs mole%  $\text{CeO}_2$  at room temperature.



transformation could be expressed as

$$K_c = \left[ K_0^2 + \frac{2V_i E_c R (|\Delta G^C| - \Delta U_{se} f)}{(1 - \nu_c^2)} \right]^{1/2}$$

where  $K_0$  is the critical stress intensity factor for the composite without the transformation toughening phenomena,  $E_c$  and  $\nu_c$  are the elastic properties of the material,  $V_i$  is the volume fraction of the phase which could undergo the stress-induced transformation,  $R$  is the size of the transformation zone adjacent to the crack and  $(|\Delta G^C| - \Delta U_{se} f)$  is the work loss per unit volume during the stress-induced transformation. Since the magnitude of the chemical free-energy change associated with the transformation,  $|\Delta G^C|$ , is expected to exhibit the greatest dependence on temperature and alloying relative to the other factors, it was predicted that the contribution of the stress-induced transformation to fracture toughness (i.e., the second term in Eq. (3)) would have the same temperature and alloy dependence as  $|\Delta G^C|$ . Based on the known temperature and alloying dependence of  $|\Delta G^C|$  for the  $ZrO_2(t) \rightarrow ZrO_2(m)$  transformation,  $K_c$  is expected to decrease with increasing temperature and alloying content which is the general result shown in Figs. 2 and 4, respectively. The following paragraphs present more detailed analysis and discussions of these data with reference to Eq. (3).

#### 4.1 Temperature Dependence

Based on the assumption that  $|\Delta G^C|$  is the only temperature dependent factor in Eq. (3), data obtained during this study and reported in Part 4<sup>2</sup> were used to calculate  $(|\Delta G^C| - \Delta U_{se} f)$  as a function of temperature for comparison





with the known temperature dependence of  $|\Delta G^C|$  for the transformation of pure  $ZrO_2$ .<sup>6</sup> This calculation started by determining the size of the transformation zone,  $R$ , for each material at room temperature, using the average room temperature value of  $(|\Delta G^C| - \Delta U_{sef})$  calculated in Part 4 for a series of  $Al_2O_3/ZrO_2$  composites, values of  $K_0$  and  $E_C$  reported\* for each material in Part 4 and room temperature  $K_C$  values reported here. Table 2 lists these values and the resulting value of  $R$  as determined by rearranging Eq. (3). It should be noted that in Part 2, it was hypothesized that  $R =$  the grain size; calculated values of  $R$  shown in Table 2 are consistent with the grain sizes of the  $ZrO_2$  phase reported for the hot-pressed materials in Part 4.

In the next step, values of  $K_C$  vs temperature reported in Table 1 and the assumed temperature independent values of  $K_0$ ,  $E_C$ ,  $v_C$ ,  $V_i$  and  $R$  reported in Table 2 were used to calculate  $(\Delta G^C - \Delta U_{sef})$  as a function of temperature for each material by rearranging Eq. (3). These results are shown in Fig. 5;\*\* Table 2 also reports the slope of each line  $(\delta(|\Delta G^C| - \Delta U_{sef})/\delta T)$  and the temperature where  $(|\Delta G^C| - \Delta U_{sef}) = 0$ ,  $(T_0)$ . The fifth line drawn in Fig. 5 is the temperature dependence of  $|\Delta G^C|$  for pure  $ZrO_2$  as previously reported by Whitney.<sup>6</sup>

The calculations shown in Fig. 5 contain three results, which adds greater confidence to the validity of the theoretical fracture mechanics calculations (Eq. (3)). First, since  $|\Delta G^C|$  is expected to exhibit the greatest temperature dependence relative to other factors in Eq. (3), the slopes of the

\*As in Part 4,  $v_C$  was assumed to be 0.25.

\*\*The four lines coincide at 25°C since it was assumed in step one that all materials had the same value of  $(|\Delta G^C| - \Delta U_{sef})$  at 25°C.



Table 2  
Values Used to Analyze  $K_C$  vs Temperature Data

Material	$K_C^*$ (MPa·m <sup>1/2</sup> )	$K_0^*$ (MPa·m <sup>1/2</sup> )	$(\Delta G^* - \Delta U_{se}^*)$ (MJ·m <sup>-3</sup> )	$E_C^*$ (GPa)	$v_C^*$	$V_i$	$R$ ( $\mu$ m)	$\frac{\partial(\Delta G^* - \Delta U_{se}^*)}{\partial T}$ (MJ·m <sup>-3</sup> + C° <sup>-1</sup> )	$T_0$ (C°)
Al <sub>2</sub> O <sub>3</sub> /29.3 v/o ZrO <sub>2</sub> (+2 m/o Y <sub>2</sub> O <sub>3</sub> ) (Hot Pressed)	7.45	4.10	188	333	0.25	0.293	0.99	-0.29	680
Al <sub>2</sub> O <sub>3</sub> /30 v/o ZrO <sub>2</sub> (+2 m/o Y <sub>2</sub> O <sub>3</sub> ) (Sintered)	8.83	4.10	188	333	0.25	0.30	1.53	-0.27	730
Al <sub>2</sub> O <sub>3</sub> /45 v/o ZrO <sub>2</sub> (+2 m/o Y <sub>2</sub> O <sub>3</sub> ) (Hot Pressed)	8.30	3.70	188	285	0.25	0.45	1.10	-0.21	900
ZrO <sub>2</sub> (+2 m/o Y <sub>2</sub> O <sub>3</sub> ) (Hot Pressed)	6.71	3.90	188	207	0.25	1.00	0.36	-0.24	830
Average of four materials									
ZrO <sub>2</sub> (pure) (6)								-0.25	785
ZrO <sub>2</sub> .96Y <sub>0.04</sub> O <sub>1.98</sub> (ZrO <sub>2</sub> + 2 m/o 1/2 O <sub>3</sub> ) (7.8)								-0.25	1200
									600 - 830°C

\*Room temperature values, Table 1  
\*Room temperature values, Part 4.

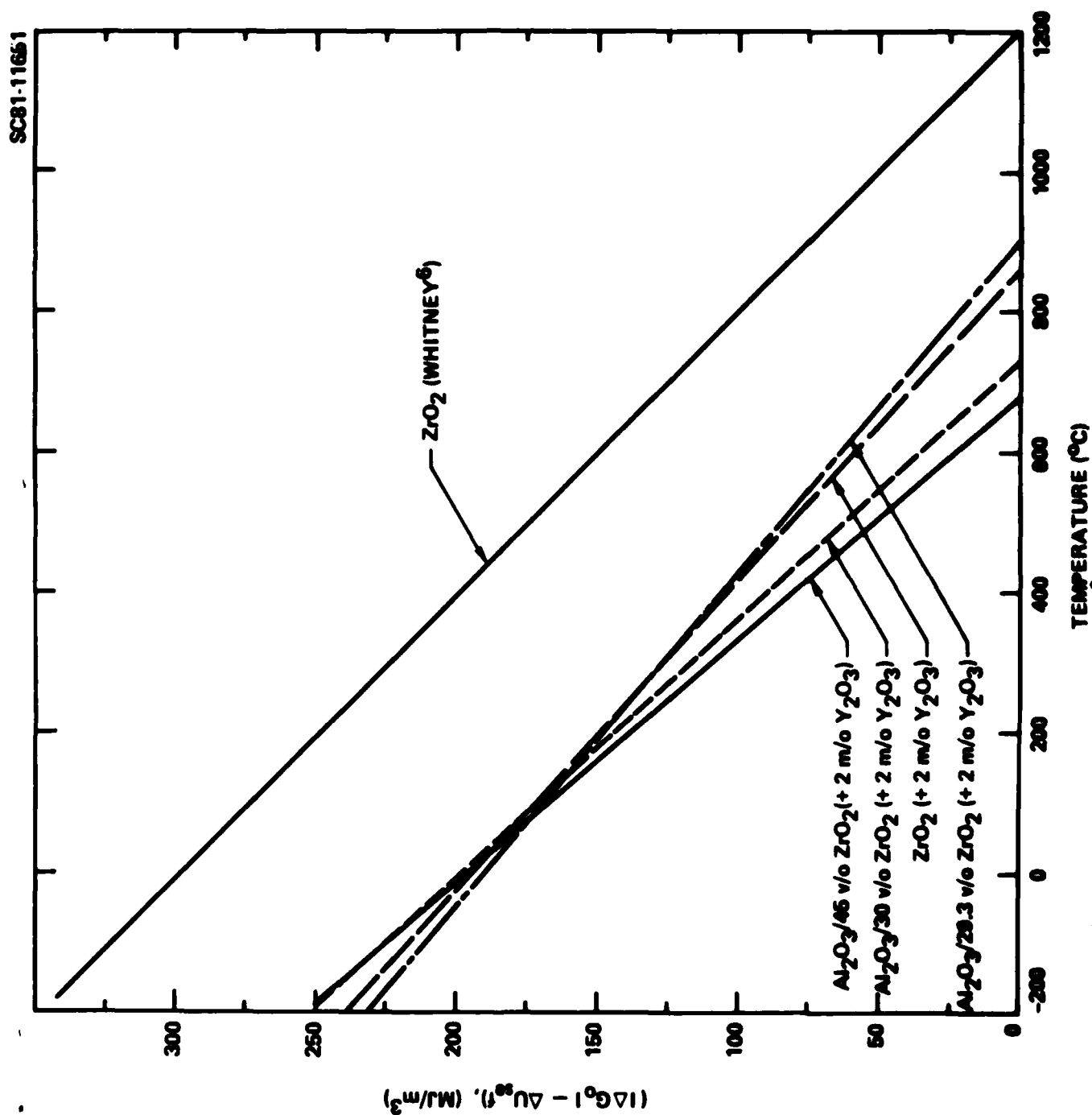


Fig. 5 Calculated values of  $(\Delta G^\circ - \Delta U^\circ)$  vs temperature for four materials studied. Upper line is  $\Delta G^\circ$  vs temperature for pure  $\text{ZrO}_2$  as



SC5117.12TR

four lines in Fig. 5 should be the same as  $\delta|\Delta G^C|/\delta T$  for  $Zr_{0.96}Y_{0.04}O_{1.98}$  ( $ZrO_2 + 2 \text{ m/o } Y_2O_3$ ). Although  $|\Delta G^C|$  vs temperature data do not exist for this solid-solution compound, it is important to note that the slopes are nearly coincident (see Table 2) for that of pure  $ZrO_2$  as reported by Whitney.<sup>6</sup> Second, the temperature ( $T_0$ ) where  $(|\Delta G^C| - \Delta U_{sef}) = 0$  lie within the range of transformation temperatures (where  $\Delta G^C = 0$ ) (see Table 2) for  $Zr_{0.96}Y_{0.04}O_{1.98}$  powder.<sup>7,8</sup> This result suggests that the residual strain energy associated with the  $ZrO_2$  grains that contribute most to the fracture toughness is very small, viz.  $\Delta U_{sef} = 0$ . Third, the slope of the lines in Fig. 5 critically depend on the value of  $R$  chosen, i.e., larger or smaller values of  $R$  would not have resulted in the good agreement with  $\delta|\Delta G^C|/\delta T$  for pure  $ZrO_2$ . Values of  $R$  calculated from room temperature data\* (Step 1) not only result in reasonable slopes for  $\delta|\Delta G^C|/\delta T$ , but they are also in good agreement with the size of the  $ZrO_2$  grains as hypothesized by theory.

#### 4.2 Effect of Alloying

Based on the assumption that  $|\Delta G^C|$  is the only factor in Eq. (3) affected by alloying  $CeO_2$  with  $ZrO_2$ , the  $K_{IC}$  results presented in Eq. (2) have been used to calculate the combined factor  $(|\Delta G^C| - \Delta U_{sef})R$ . The linear expression resulting from combining Eq. (2) and (3) with the appropriate values<sup>2</sup>

\*A second approach can also be used to determine  $R$  for each material by calculating the combined product  $R(|\Delta G^C| - \Delta U_{sef})$  in Eq. (3) as a function of temperature and assuming that  $\delta(|\Delta G^C| - \Delta U_{sef})/\delta T = 0.248 \text{ MJ}\cdot\text{m}^{-3} \cdot \text{C}^{-1}$  (the value of  $\delta|\Delta G^C|/\delta T$  for pure  $ZrO_2$ ).<sup>6</sup> Using this approach, values of  $R$  for the four materials listed in Table 2 are 1.2  $\mu\text{m}$ , 1.65  $\mu\text{m}$ , 0.95  $\mu\text{m}$  and 0.34  $\mu\text{m}$ , respectively.



$K_0 = 4.1 \text{ MPa m}^{1/2}$ ,  $E_0 = 333 \text{ GPa}$ ,  $\nu_c = 0.25$  and  $V_f = 0.30$  for the  $\text{Al}_2\text{O}_3/30 \text{ v/o}$   $\text{ZrO}_2$  (+  $\text{CeO}_2$ ) compositions is

$$(|\Delta G^C| - \Delta U_{sef})R = (415 - 15.8 M) \text{ MJ/m}^2 \quad (4)$$

Equation (4) can be used to estimate two thermodynamic properties of  $\text{ZrO}_2$ , which again adds greater confidence to the fracture mechanisms theory as expressed in Eq. (3). First, by extrapolating the data obtained between  $M = 12$  to  $20 \text{ m/o CeO}_2$  to  $M = 0$ , one obtains the value of  $(|\Delta G^C| - \Delta U_{sef})R = 415 \text{ MJ/m}^2$  for pure  $\text{ZrO}_2$ . By choosing  $R = 1.5 \text{ }\mu\text{m}$ , the value determined to be consistent with the  $K_c$  vs temperature data for a similar, sintered  $\text{Al}_2\text{O}_3/30 \text{ v/o ZrO}_2$  composite discussed in the last section, one obtains  $(|\Delta G^C| - \Delta U_{sef}) = 275 \text{ MJ/m}^3$ . It is interesting to note that this value agrees almost exactly with the room temperature value of  $|\Delta G^C| = 290 \text{ MJ/m}^3$  for pure  $\text{ZrO}_2$  as previously calculated by Whitney (see Fig. 5). Although this near perfect agreement may be fortuitous, it again suggests that the residual strain energy ( $\Delta U_{sef}$ ) associated with the transformed grains adjacent to the crack surfaces can be neglected in estimating their contribution to fracture toughness.

Second, previous phase equilibria work<sup>5</sup> in the  $\text{ZrO}_2\text{-CeO}_2$  binary system has suggested that  $\text{CeO}_2$  additions in the range between 15 to 20 m/o  $\text{CeO}_2$  lowers the tetragonal  $\rightarrow$  monoclinic transformation temperature below  $25^\circ\text{C}$ .  $K_c$  measurements (see Fig. 2) clearly show that the tetragonal phase contributes to toughening over the complete range of  $\text{CeO}_2$  studied (11 m/o to 22 m/o). That is,  $K_c$  measurements strongly suggest that the eutectoid temperature is  $> 25^\circ\text{C}$ . Using the fracture mechanics data, one can estimate the eutectoid temperature by



assuming that  $\Delta U_{sef} = 0$  and determining the value of  $M$  in Eq. (4) where  $|\Delta G^C|R = 0$ . This condition exists when  $M = 26$  m/o  $CeO_2$ . By constructing a line between  $1200^\circ C$  and  $26$  m/o  $CeO_2$  on the  $ZrO_2$ - $CeO_2$  phase diagram and recognizing that the tetragonal + cubic phase field exists when  $M > 20$  m/o  $CeO_2$ , one estimates the eutectoid temperature as  $270^\circ C$  which alters the phase diagram shown in Fig. 1 to that shown in Fig. 6.

## 5.0 CONCLUSIONS

1. The fracture toughness of materials containing tetragonal  $ZrO_2$  decreased with increasing temperature and alloying addition, consistent with theoretical predictions.
2. An analysis of the data suggests that the residual strain energy associated with the transformed  $ZrO_2$  grains can be neglected. Thus, the equation which appears to explain the contribution of the stress-induced phase transformation to fracture toughness can be rewritten as

$$K_C = \left[ K_0^2 + \frac{2|\Delta G_C|E_C V_1 R}{(1 - \nu_C^2)} \right]^{1/2} \quad (5)$$

3. The fracture mechanics data, when analyzed with respect to theory as expressed by Eq. (3), best fit the thermodynamic data for  $ZrO_2$  when it was assumed that the size of the transformation zone is the same size as the  $ZrO_2$  grains.

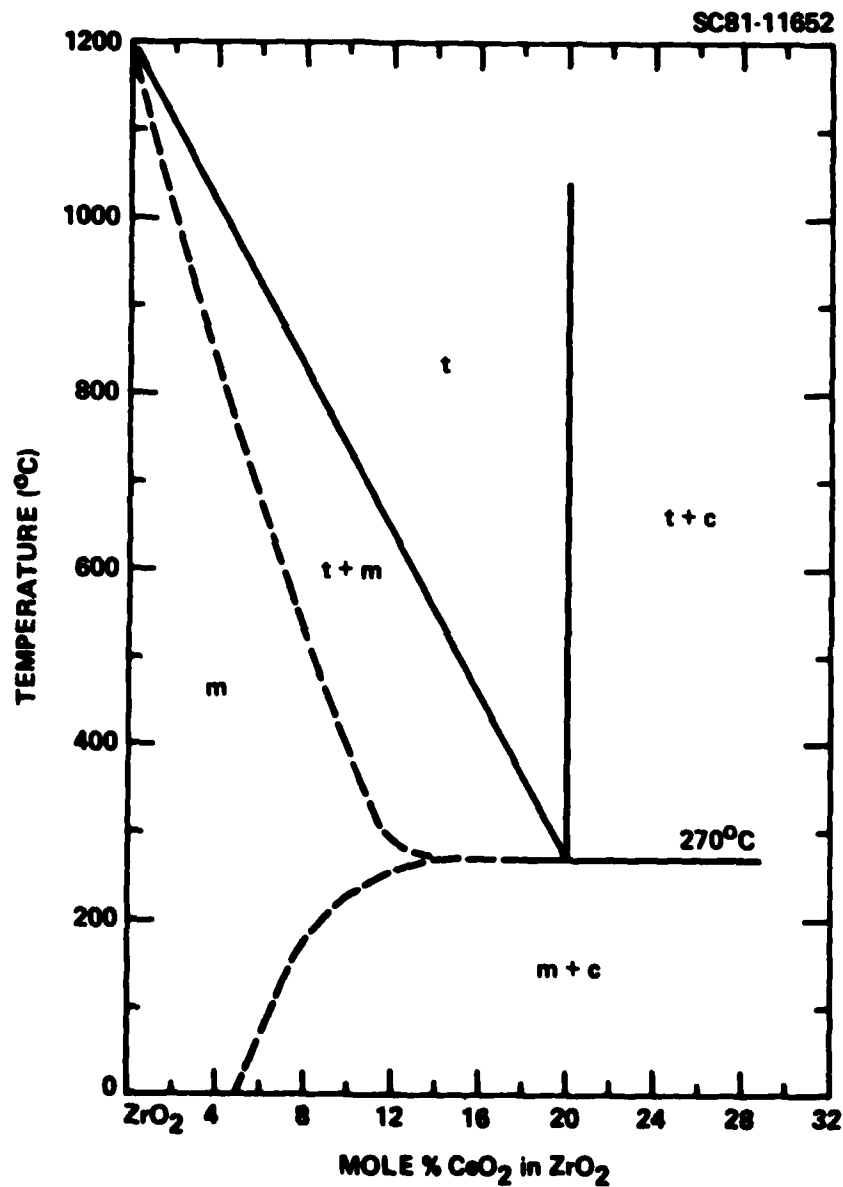


Fig. 6 A portion of the ZrO<sub>2</sub>-CeO<sub>2</sub> phase diagram, in which the eutectoid temperature has been estimated through fracture mechanics data.

**DAT  
FILM**



